Supplementary Material for:

DNA damage checkpoint dynamics drive cell cycle phase transitions

Hui Xiao Chao[1,2], Cere E. Poovey[1], Ashley A. Privette[1], Gavin D. Grant[3,4], Hui Yan Chao[1], Jeanette G. Cook[3,4], and Jeremy E. Purvis[1,2,4,†]

[1]Department of Genetics
[2]Curriculum for Bioinformatics and Computational Biology
[3]Department of Biochemistry and Biophysics
[4]Lineberger Comprehensive Cancer Center

University of North Carolina, Chapel Hill
120 Mason Farm Road
Chapel Hill, NC 27599-7264

[†]Corresponding Author:
Jeremy Purvis
Genetic Medicine Building 5061, CB#7264
120 Mason Farm Road
Chapel Hill, NC 27599-7264
jeremy_purvis@med.unc.edu

Model simulations and parameter fitting

All simulations and parameter fitting were performed using MATLAB. The durations of each cell cycle phase—G1, S, or G2-M—under basal conditions were fitted to an Erlang distribution (**Figure S3**, upper panels). The Erlang distribution was chosen for three main reasons. First, it contains two independent parameters, the minimal number of parameters needed to describe distributions of varying mean and variance. Second, the Erlang distribution has a simple and relevant biological interpretation: each cell cycle phase can be viewed as a multistep biochemical process that needs to be completed sequentially in order to advance to the next cell cycle phase. Alternatively, the multistep process can be viewed as the accumulation of a clock protein whose number needs to exceed a certain threshold value before transitioning to the next cell cycle phase. Third, the Erlang distribution provides a framework that is amenable for carrying out stochastic simulations that are biologically interpretable. In particular, the time step of simulation corresponds to the duration of the current subphase. This framework is also flexible to modifications of the checkpoint dynamics, such as implementing an all-or-none or graded slowdown, as well as introducing a temporally located commitment point within a particular cell cycle phase.

For each cell cycle phase, by fitting the experimental distribution of cell cycle phase durations, we obtained two parameters: shape (k)—which can be interpreted as the number of steps within a cell cycle phase—and scale (1/λ)—which can be interpreted as the average timescale for each of the steps. After the fitting, we obtained 2 parameters for each cell cycle phase and each cell line. Using the estimated parameters, we were able to simulate the cell cycle phase transitions in an asynchronous population with phase durations drawn from the distribution under basal conditions. In the following, we will use G1 as an example, but the same method was applied to each cell cycle phase. Because the Erlang distribution is a special case of the Gamma distribution with integer scale parameter, we can generate the phase durations from a gamma distribution in MATLAB (**Figure S3**, lower panels):

$$T_{G1,total} = \sim Gamma(k, \lambda)$$

Fitting with the "arrest-and-restart" checkpoint model:

Under the arrest-and-restart checkpoint model, the checkpoint implements a complete halt and a permanent arrest probability. Therefore, we incorporated these two properties by introducing two free parameters: delay duration (μ), which was drawn from a normal distribution with standard deviation proportional to the mean, and a permanent arrest probability (p_{arrest}), into our simulations.

$$T_{G1,total} = \begin{cases} \sim Gamma(k, \lambda) + t_{halt}\,, & \text{with probability } (1 - p_{arrest}) \\ \infty, & \text{with probability } p_{arrest} \end{cases}$$

where

$$t_{halt} \sim Gaussian(\mu, \mu/3)$$

To simulate cell cycle phase progression in asynchronous cells, we generate a random variable *f* from 0 to 1 to indicate the proportion of cell cycle phase already completed at the time of damage:

$$f \sim Uniform(0, 1)$$

With this *f*, we could then generate the post-damage transition time needed for the transition curves:

$$T_{G1,post-damage} = \begin{cases} \sim Gamma(k, \lambda) \times (1 - f) + t_{halt}\,, & \text{with probability } (1 - p_{arrest}) \\ \infty, & \text{with probability } p_{arrest} \end{cases}$$

We then estimated these two parameters (μ, p_{arrest}) by comparing the simulated transition curve of the model with the experimental data. We used the *fminsearch* function in MATLAB to minimize the mean square difference between the simulation and experimental data in a brute-force approach.

Fitting with the refined checkpoint model:

All-or-none kinetics:

In addition to delay duration (μ) and permanent arrest probability (p_{arrest}), as in the arrest-and-restart checkpoint model, we introduced an additional free parameter—commitment point l_{cp}—to allow for checkpoint escape once the cell cycle phase progression passes that temporally located commitment point.

If $f \leq l_{cp}$:

$$T_{G1,total} = \begin{cases} \sim Gamma(k,\lambda) + t_{halt}\,, & \text{with probability } (1 - p_{arrest}) \\ \infty, & \text{with probability } p_{arrest} \end{cases}$$

Then, the post-damage transition time would be:

$$T_{G1,post-damage} = \begin{cases} \sim Gamma(k,\lambda) \times (1-f) + t_{halt}\,, & \text{with probability } (1 - p_{arrest}) \\ \infty, & \text{with probability } p_{arrest} \end{cases}$$

If $f > l_{cp}$:

$$T_{G1,total} \sim Gamma(k,\lambda)$$

Then, the post-damage transition time would be:

$$T_{G1,post-damage} = \sim Gamma(k,\lambda) \times (1-f)$$

Graded slowdown kinetics:

In addition to the above framework that described an all-or-none kinetics, we also performed simulation under the graded slowdown kinetic by allowing the scale parameter (from the fitted Erlang distribution), which related to the rate of progression under basal conditions, to change. Under this graded-slowdown model, we removed the halt duration parameter (μ), and introduced an additional parameter, the new scale, or the phase progression rate after damage (λ_{slow}), to represent the slowed rate after damage.

$$T_{G1,before-damage} \sim Gamma(k,\lambda) \times f$$

If $f \leq l_{cp}$:

$$T_{G1,post-damage} = \begin{cases} \sim Gamma(k,\lambda_{slow}) \times (1-f)\,, & \text{with probability } (1 - p_{arrest}) \\ \infty, & \text{with probability } p_{arrest} \end{cases}$$

If $f > l_{cp}$:

$$T_{G1,post-damage} = \sim Gamma(k,\lambda) \times (1-f)$$

Then, the total phase duration would be:

$$T_{G1,total} = T_{G1,before-damage} + T_{G1,post-damage}$$

Although we performed the stochastic simulations under the framework of an Erlang process, it is important to note that the conclusions should be robust to the model framework that we chose. For example, for the all-or-none checkpoint kinetics, the halt durations in G2-M were apparent in the plateau region of the transition curve and did not depend on whether it was an Erlang process. For the graded slowdown checkpoint kinetics in S phase, the slowed cell cycle phase progression could be estimated by calculating the slope as in **Figure 6B**, which is independent of the model framework. These parameters could be estimated under a deterministic framework. However, the Erlang process provided an easy and trackable framework to carry out the stochastic simulations with modifications upon DNA damage.

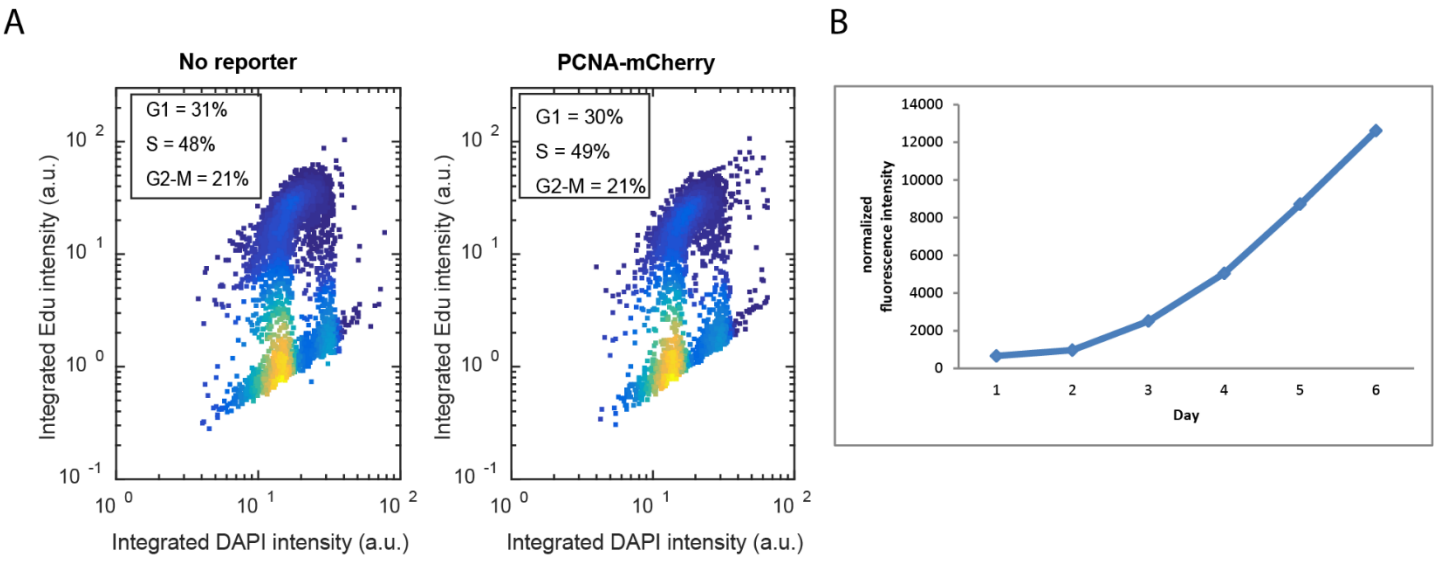

Figure S1. Cell cycle progression is not disturbed by the live cell reporter.

A. Cell cycle distribution of U2OS cells. Cells with (left panel) and without (right panel) the expression of PCNA-mCherry were pulsed with 10 μM EdU for 1 hour, followed by fixation, staining, and quantification for EdU incorporation and DAPI content. (n>1800)

B. The doubling time of the cell line in culture was consistent with the cell cycle durations measured from live-cell image. The doubling time (20.1 hours) of U2OS cells expressing the PCNA-mCherry reporter was measured by fitting the most rapid phase of the growth curve with an exponential function. Relative cell count was quantified using the CellTiter blue assay.

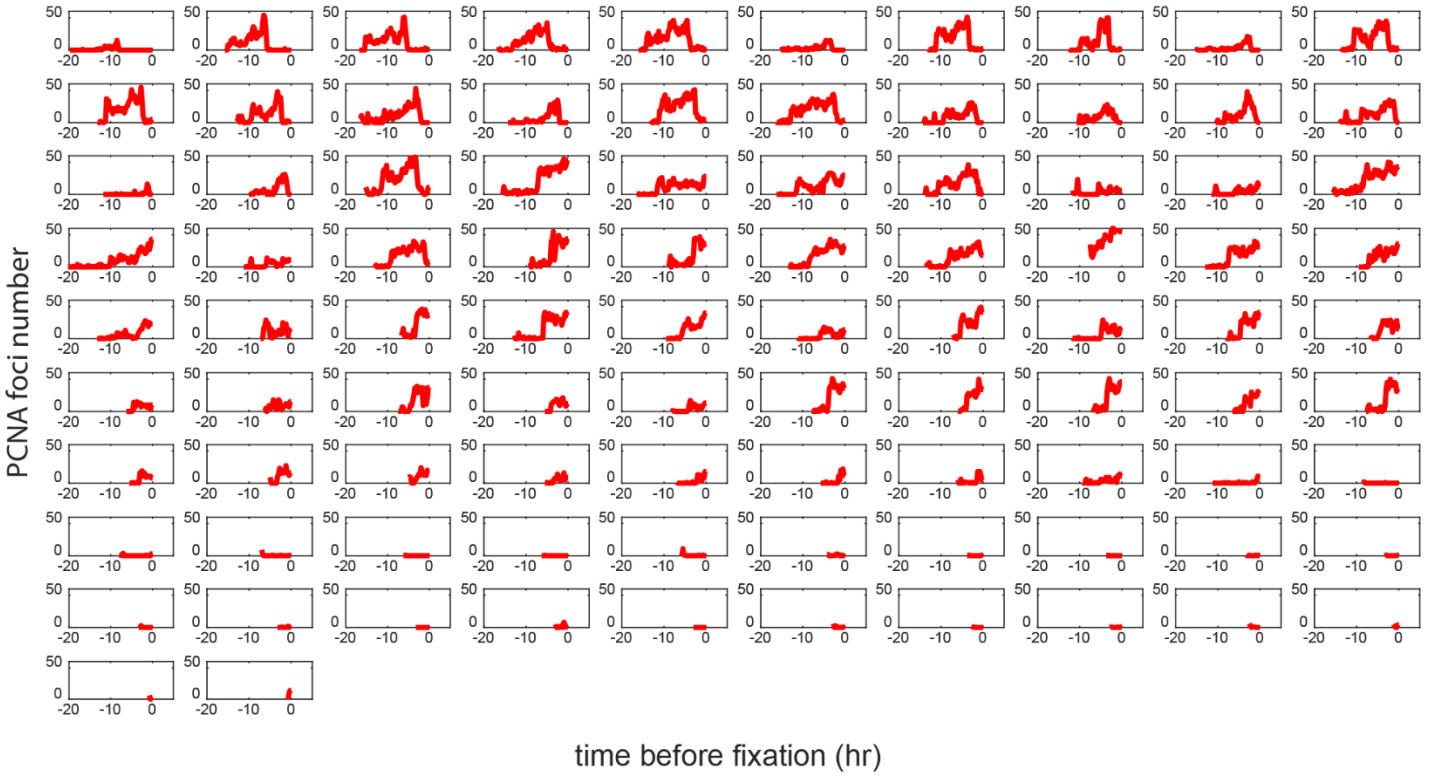

Figure S2. Trajectories of PCNA foci number

Live cell imaging of U2OS cells expressing the PCNA-mCherry reporter. Asynchronously cycling cells were imaged for 24 hours, and the number of PCNA foci in each cell was quantified every 15 minutes. Data were acquired from **Figure 2E**, but were plotted as line graphs instead of a heatmap. The single cell trajectories are shown in the order of Cell ID in **Figure 2E** from left to right and from top to bottom.

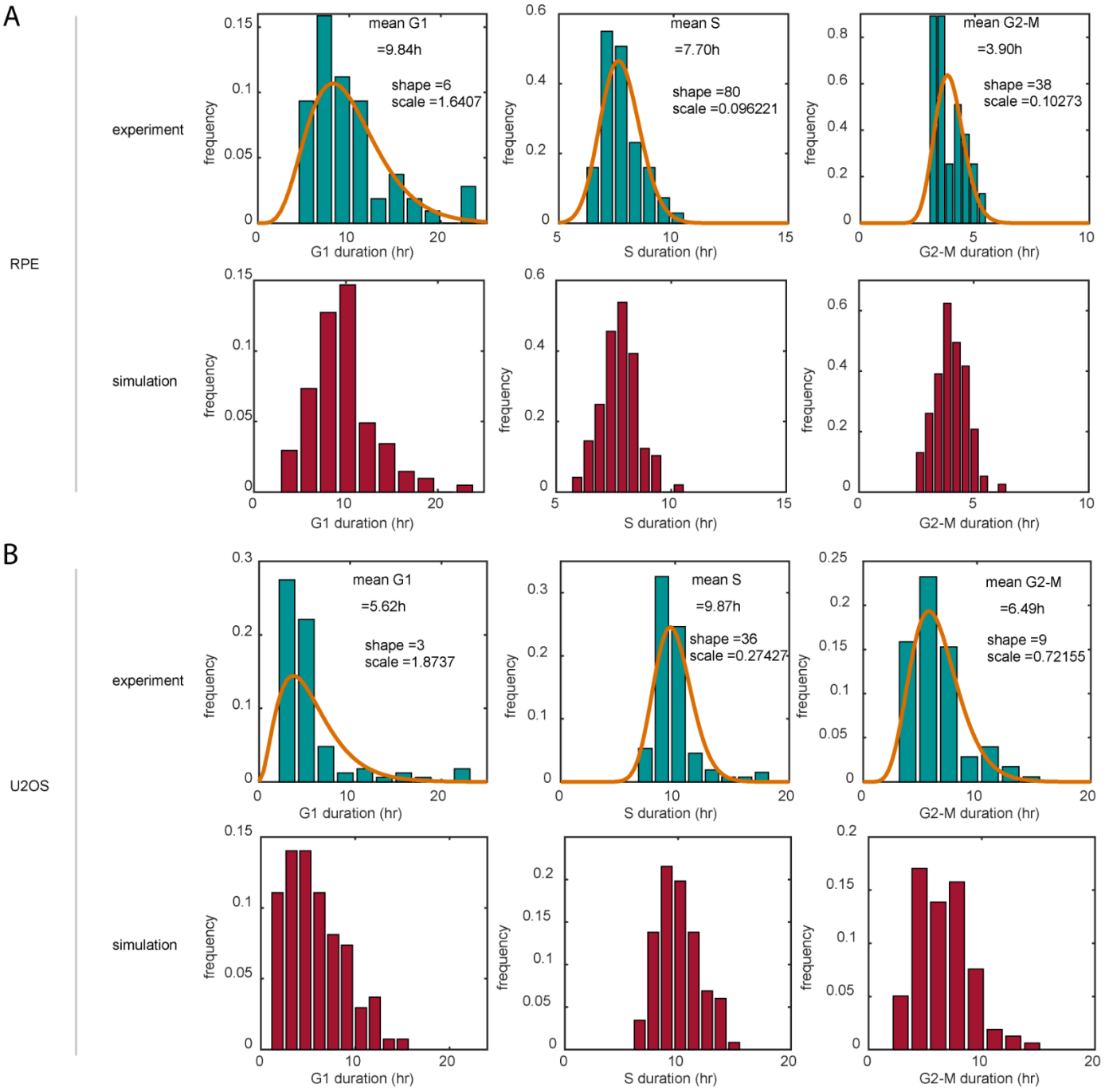

Figure S3. Cell cycle phase distribution fitted with Erlang distributions.

A-B. Top panels: Asynchronously proliferating RPE (A) and U2OS (B) cells were quantified for their cell cycle phase (G1, S, G2-M) durations based PCNA-mCherry morphology using time-lapse microscopy. The distributions of the cell cycle phase were fitted with Erlang distributions to estimate the shape (*k*) and scale (1/λ) parameters. Bottom panels: simulations of cell cycle phase durations based on the fitted Erlang distribution parameters. n>60, except for RPE G2-M n=26.

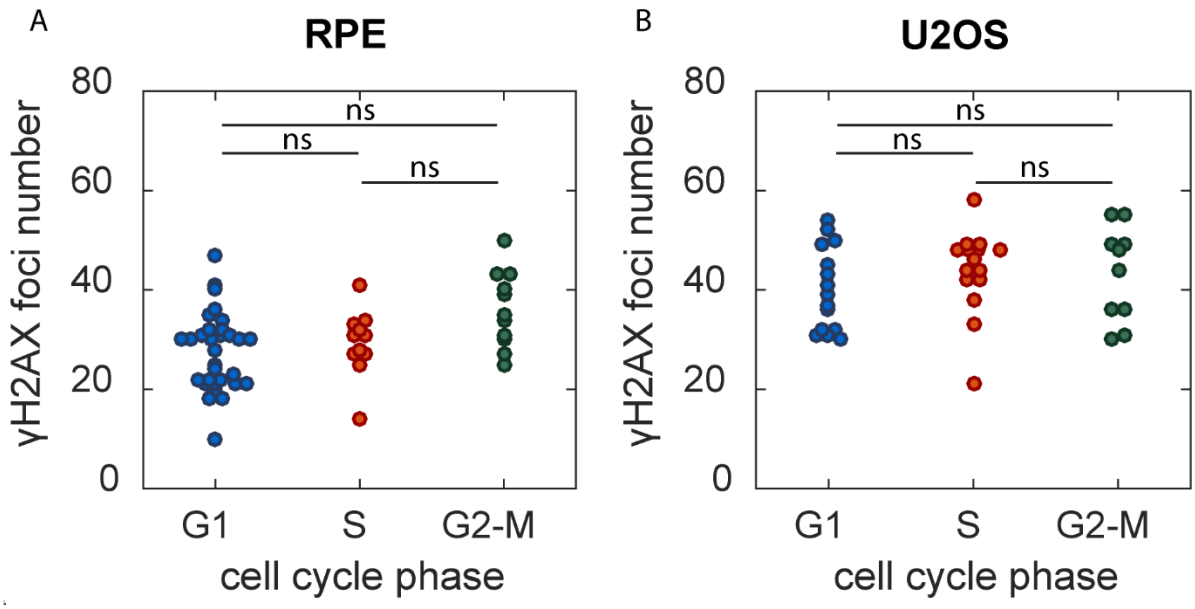

Figure S4. The amounts of DSBs induced by NCS were similar in each cell cycle phase.

(A) RPE and (B) U2OS cells were induced with 100 ng/mL and 300 ng/mL NCS, respectively, for 30 minutes, and pulsed with 10 μM EdU for 15 minutes before fixation. The cells were then stained for γH2AX and DAPI to quantify the level of DSBs and DNA content, respectively. The cell cycle phase was designated based on the EdU and DAPI intensity. ns indicates no significant difference, based on the significance level of p=0.05 using Kolmogorov–Smirnov test.

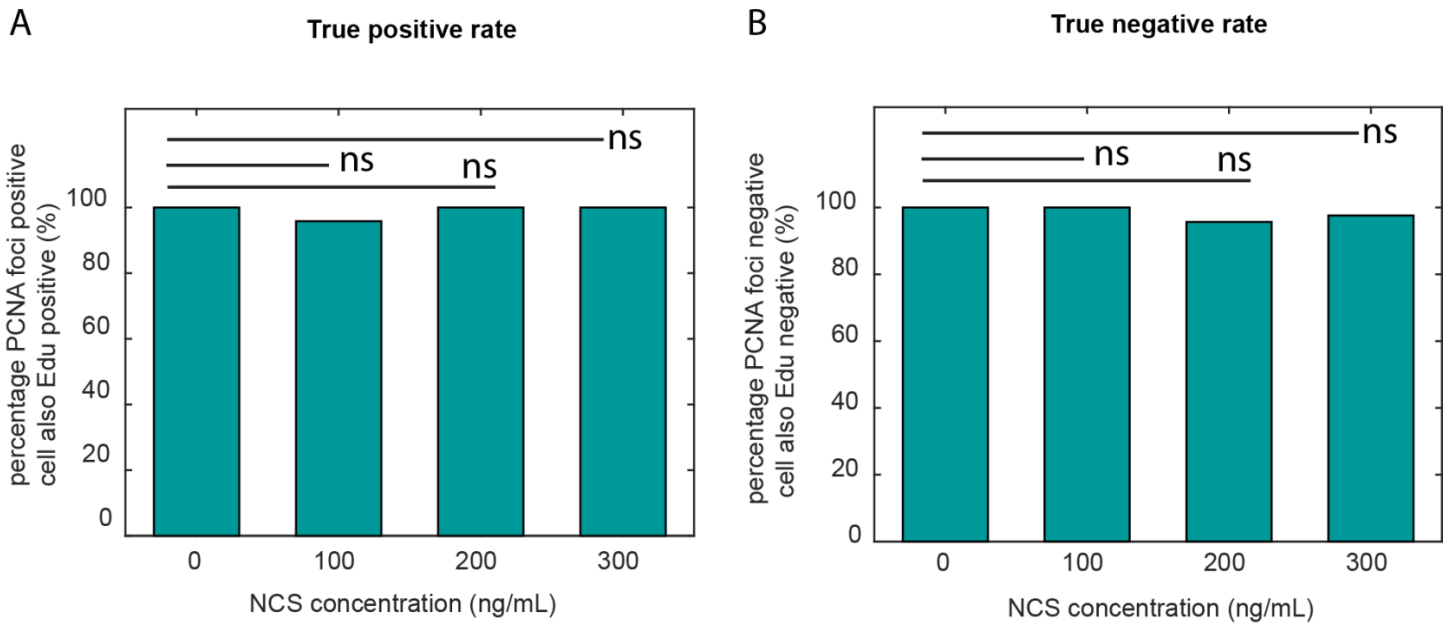

Figure S5. PCNA-mCherry is a good S phase reporter after DNA damage induced by NCS.

A-B. The true positive rate (A) and true negative rate (B) of the PCNA foci as a marker for S phase, measured by EdU incorporation. U2OS cells were treated with NCS of indicated concentrations under live-cell imaging conditions to quantify for PCNA foci. 10 hours after the treatment, the cells were pulsed with 10 μM EdU for 20 mins, followed by fixation, staining, and scoring for EdU incorporation. ns indicates no significant difference based on the significance level of p=0.05 using Fisher's exact test. In addition, DNA damage-induced PCNA foci in G1 or G2 were not observed under our conditions, which could cause the cells to be erroneously scored as having entered S phase. (n>65)

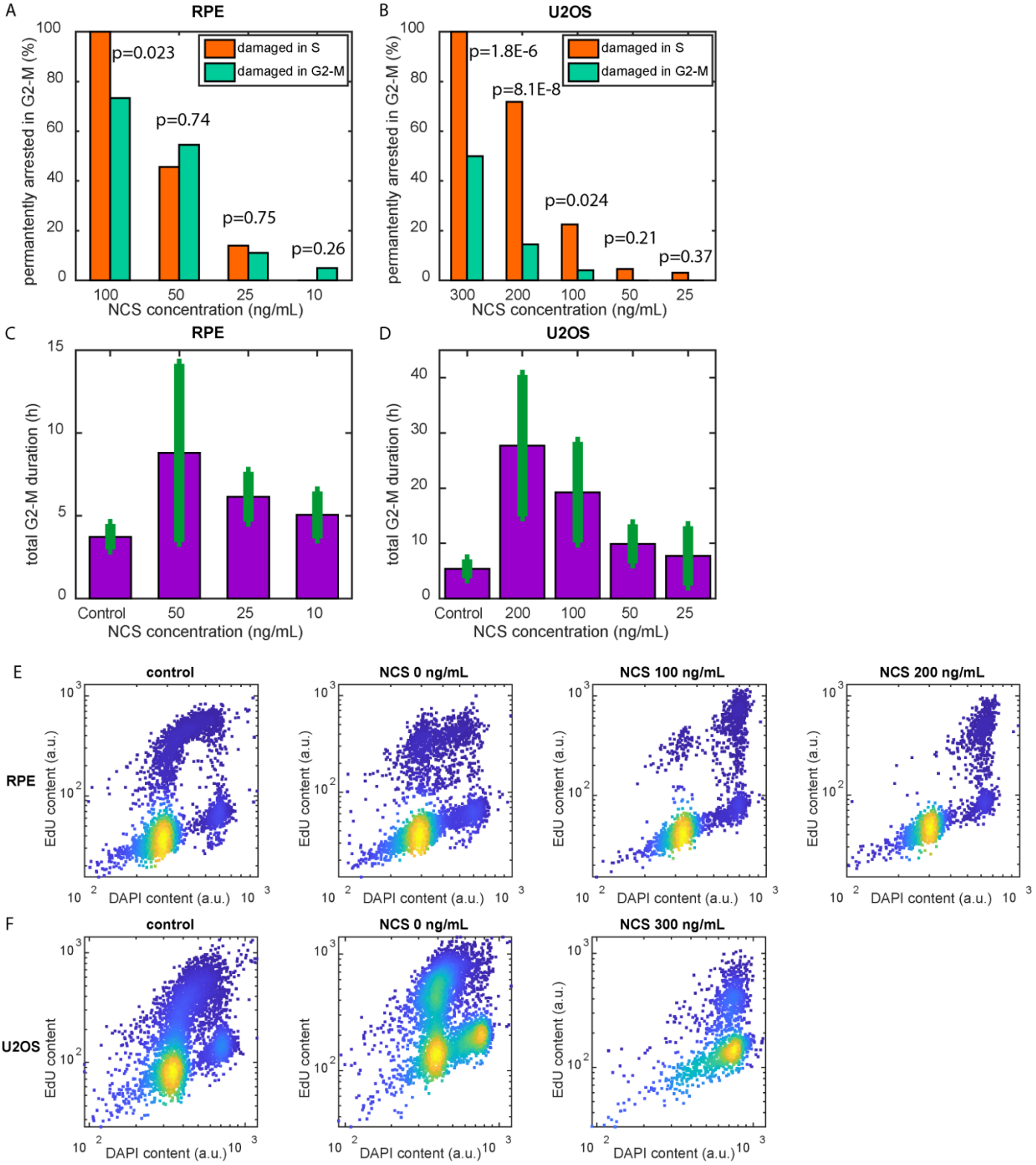

Figure S6. Cells damaged in S phase were arrested in the subsequent G2 phase.

A-B. RPE (A) and U2OS (B) cells that were damaged in S and G2-M were quantified for the fractions of being arrested in G2-M by the end of 48hr hour post damage. The p-values were calculated based on Fisher's exact test.

C-D. RPE (C) and U2OS (D) cells that were damaged in S and completed the subsequent G2-M were quantified for the G2-M durations. Control represents cells without NCS treatment. Error bars represent standard deviations.

E-F. Measuring the fate of cells damaged in S phase. RPE (E) and U2OS (D) cells were treated with NCS of indicated concentrations for 5 mins, followed by a pulse of 10 μM EdU for 25 mins, and then washed out with fresh media. The cells were then incubated for 20 hours to allow for cell cycle progression before fixation, staining, and quantification for EdU incorporation and DAPI content. The cells in the control were not treated with NCS and were pulsed with 25 minutes of EdU right before fixation to reveal the cell cycle distribution in unperturbed cells. (n ranges from 1300 to 5000)

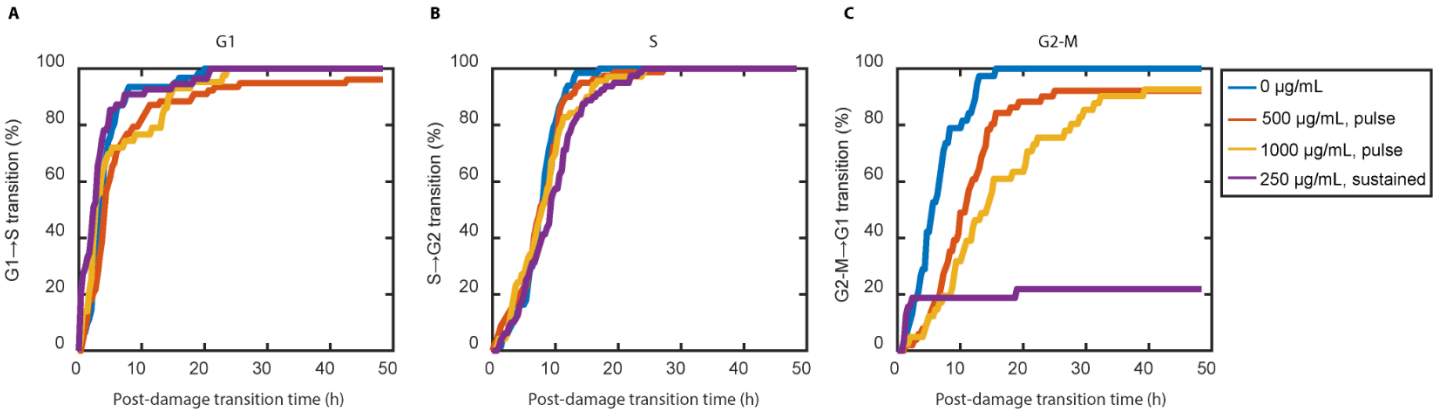

Figure S7. Transition curve as a function of cell cycle phase in response to zeocin.

A-C. Cell cycle phase-specific transition curves in response to zeocin damage in U2OS cells. Transition curves for asynchronously dividing U2OS cells treated with either a 10-minute pulse of zeocin at 500 µg/mL and 1000 ug/mL or sustained zeocin at 250 µg/mL during (A) G1, (B) S, or (C) G2-M. The pulse treatment was used to generate the transient DNA damage effect as NCS. The sustained treatment was used to generate long-term DNA damage.

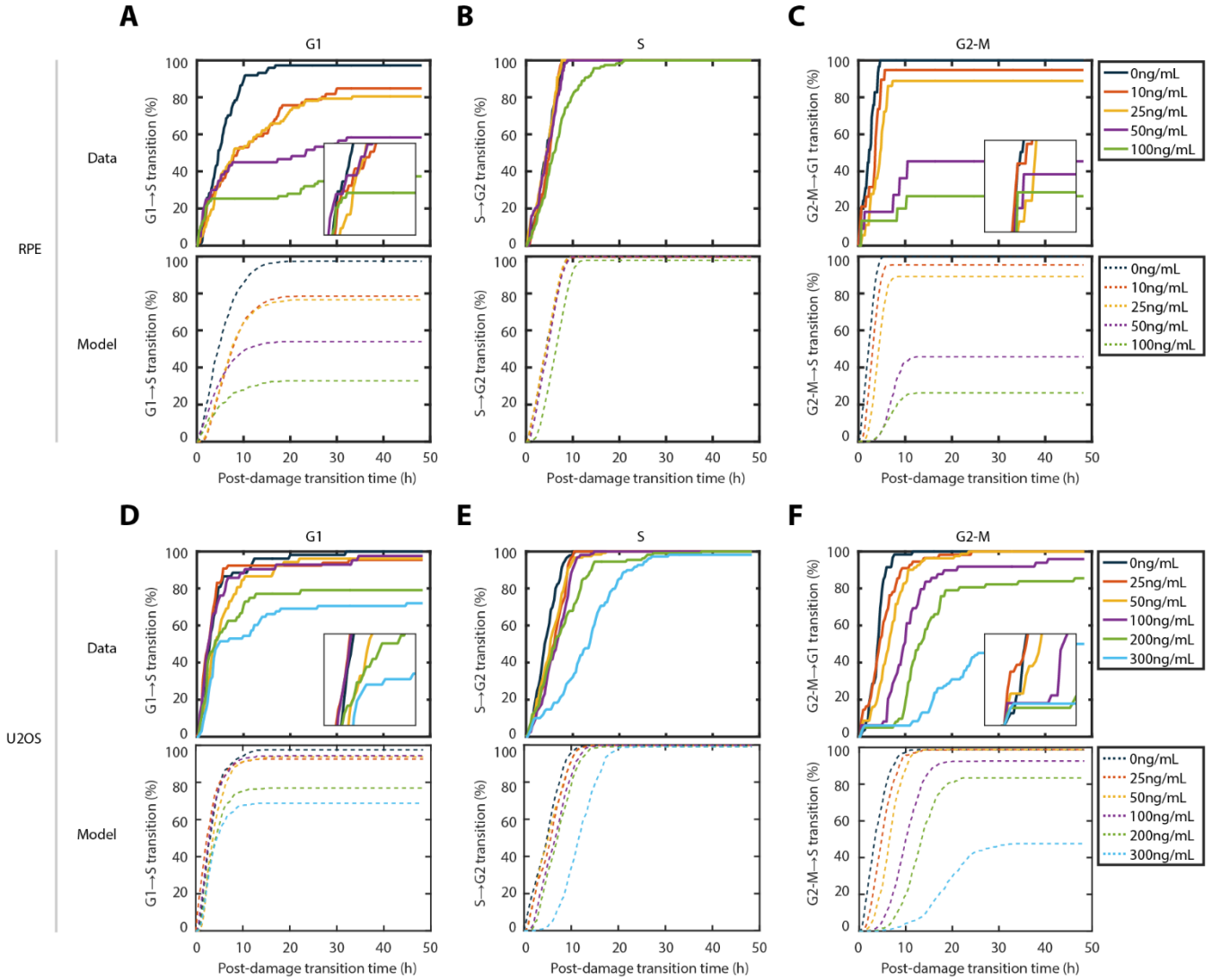

Figure S8. Cell cycle phase-specific transition curves fit with the "arrest-and-restart" model.

A-C. Cell cycle phase-specific transition curves in response to acute DNA damage in RPE cells. *Upper panels and solid lines*: As in **Figure 3A-B**, transition curves for asynchronously dividing RPE treated with NCS at the indicated concentrations during (A) G1, (B) S, or (C) G2-M. *Lower panels and dashed lines*: Best fit lines of the experimental data to the "arrest-and-restart" DNA damage checkpoint model described in **Figure 1A.**

D-F. Corresponding experimental data and model fitted curves for U2OS cells as described in panels A-C.

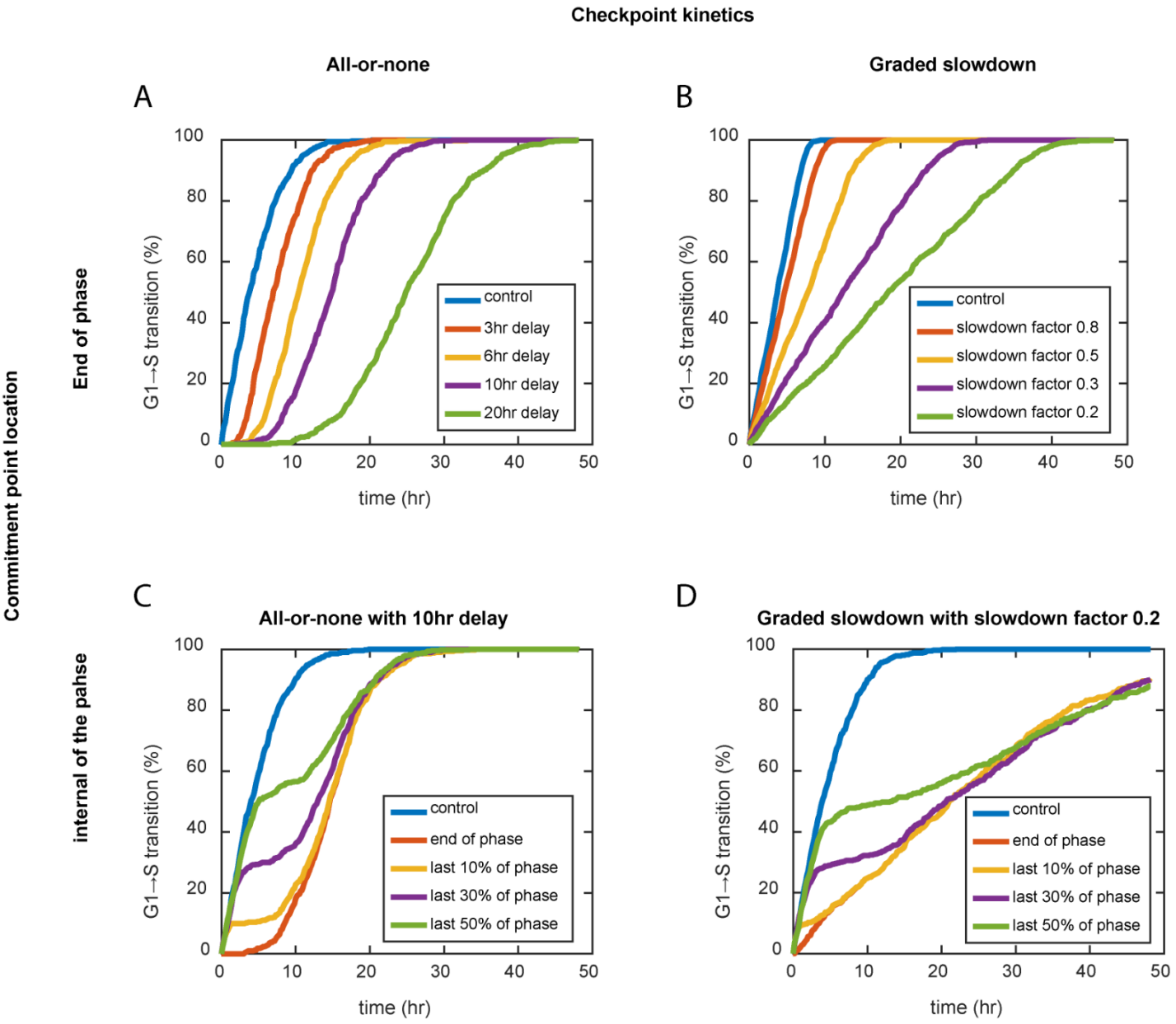

Figure S9. Each cell cycle phase implements a distinct DNA damage checkpoint response.

A-B. Simulation of cell cycle transition dynamics upon DNA damage under (A) all-or-none kinetics with varying halt duration, or (B) graded slowdown kinetics with varying slowdown factor.

C-D. Simulation of the cell cycle transition dynamics as in A and B, but incorporating the commitment point at varying locations.

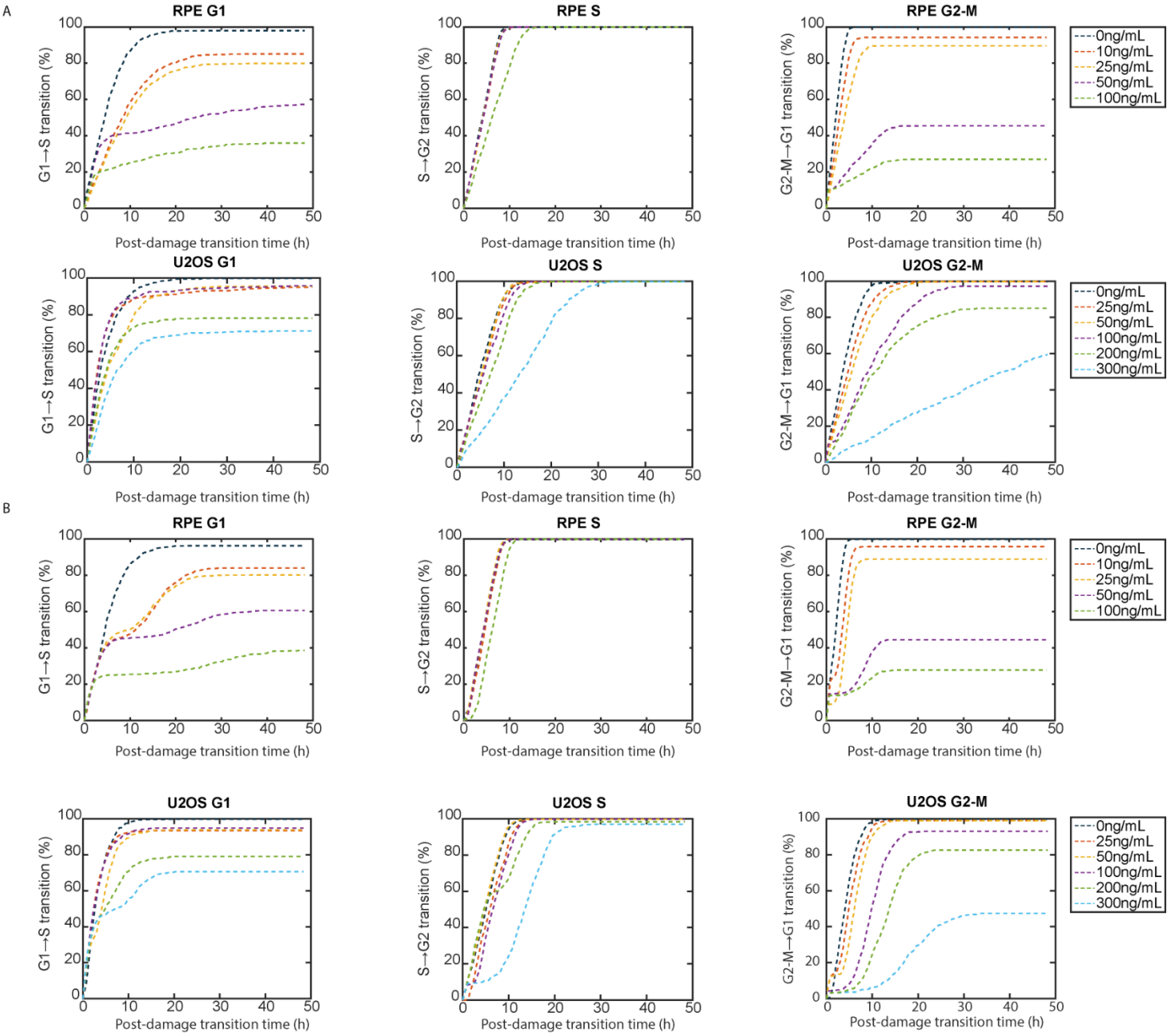

Figure S10. Model fitting of cell cycle phase-specific transition curves in response to acute DNA damage, as in lower panels of **Figure 3**, but fit with the refined model that incorporated both the flexible commitment point location and the possibility of graded slowdown checkpoint kinetics. Each condition was fit with the (A) graded slowdown or (B) all-or-none checkpoint kinetics.

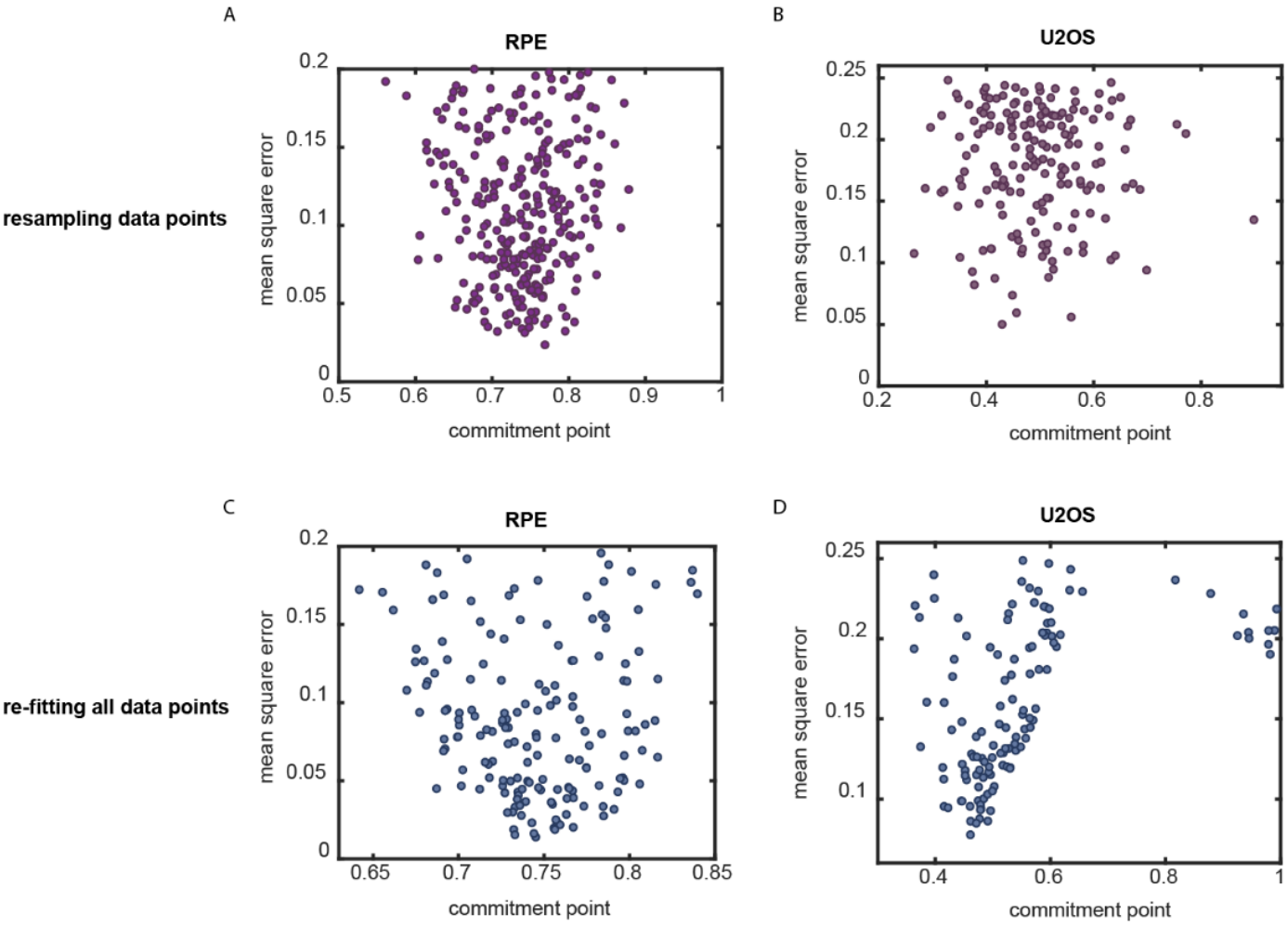

Figure S11. Model estimations of the checkpoint commitment point.

A. Commitment point estimation by resampling half of the transition data. The transition time points for RPE's G1 transition curve under 100 ng/mL NCS treatment were repeatedly and randomly drawn using half of the data points (n=51) and were fitted with the refined all-or-none checkpoint model. Estimated parameters that produced a simulated transition curve with a mean square error less than 0.2 from the experimental data were recorded (n=294).

B. Same as A, but with U2OS's G1 transition curve under 300 ng/mL NCS and half sample size of 31. Estimated parameters that produced a simulated transition curve with a mean square error less than 0.25 from the experimental data were recorded (n=181).

C. Commitment point estimation by repeated fitting using all of the transition data. The transition time points for RPE's G1 transition curve under 100 ng/mL NCS treatment were repeatedly fitted with the refined all-or-none checkpoint model. Estimated parameters that produced a simulated transition curve with a mean square error less than 0.2 from the experimental data were recorded (n=166).

D. Same as C, but for U2OS's G1 transition curve under 300 ng/mL NCS. Estimated parameters that produced a simulated transition curve with a mean square error less than 0.25 from the experimental data were recorded (n=126).

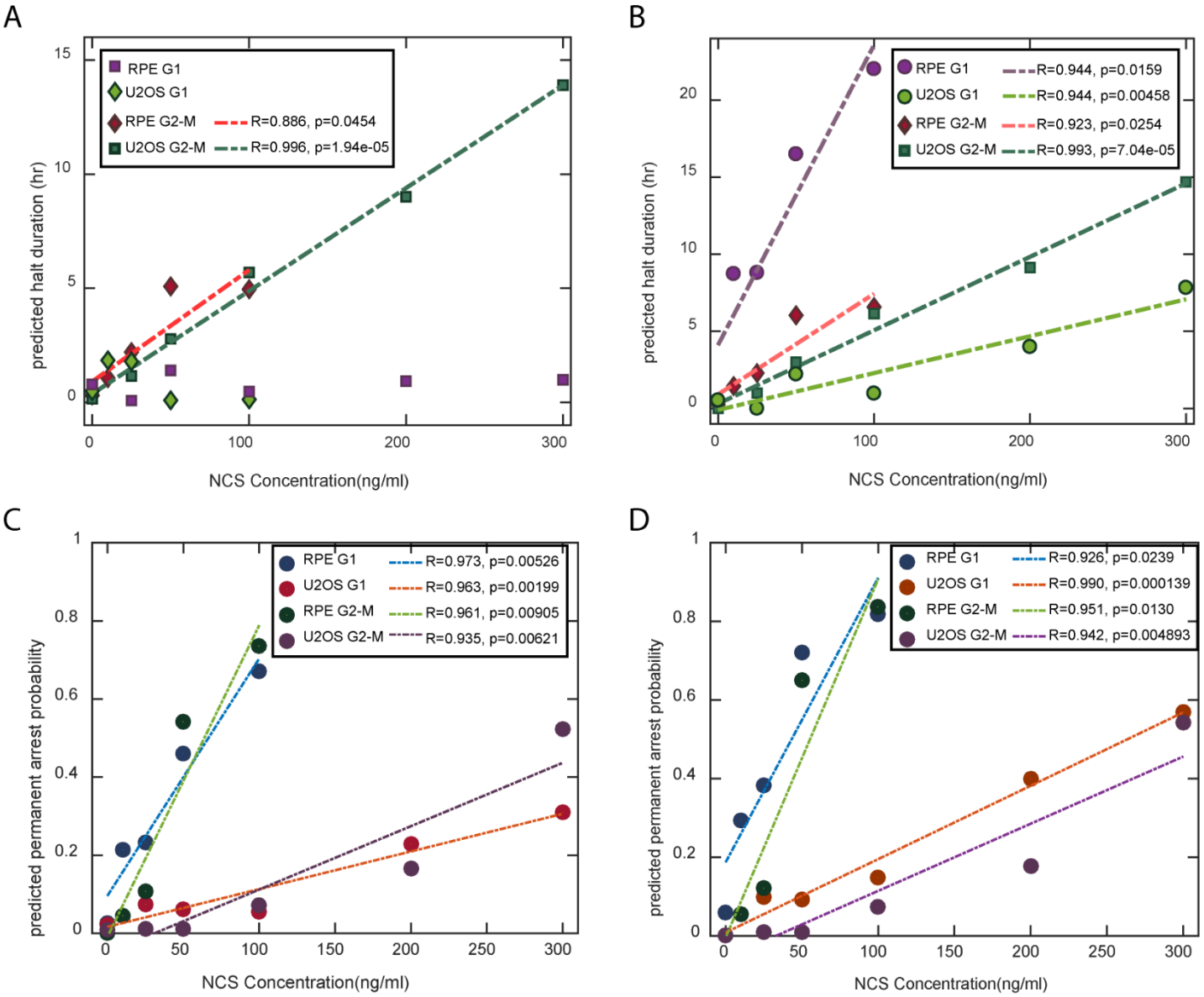

Figure S12. Model estimations of the checkpoint halt duration and permanent arrest probability as a function of DNA damage level.

A. By fitting the data with the “arrest-and-restart” model, we estimated the halt durations in G1 and G2-M in response to the indicated NCS concentrations.

B. Same as A, but the data were fitted with the refined model with a flexible commitment point.

C. By fitting the data with the “arrest-and-restart” model, we estimated the permanent arrest probabilities in G1 and G2-M in response to the indicated NCS concentrations.

D. Same as C, but the data were fitted with the refined model with a flexible commitment point.

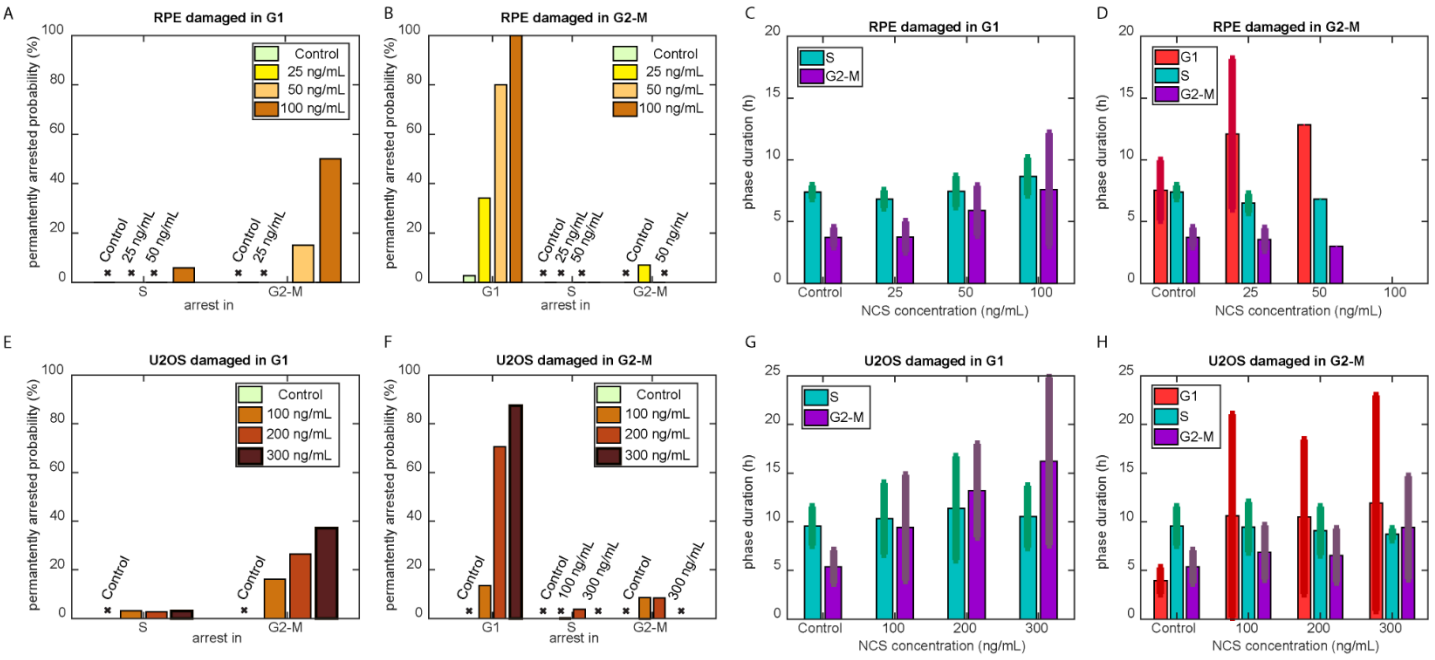

Figure S13. Cell fate after passing the cell cycle phase transition upon high DNA damage.

A-B. RPE cells damaged in (A) G1 and (B) G2-M that eventually transitioned to the next phase were quantified for the probability of being arrested in the subsequent phases by the end of the 48-hour experiment. The probability of permanent arrest in a given phase was conditioned on the cells that had entered that given phase. The “x” symbols indicate 0% permanent arrest.

C-D. RPE cells damaged in (C) G1 and (D) G2-M and completed the subsequent cell cycle phases were quantified for the phase durations. (C) For cells damaged in G1, the subsequent S (n= 42, 22,16) and G2-M (n=40, 17, 5) durations were quantified. (D) For cells damaged in G2-M, the G1 (n=22, 1, 0), S (n=16, 1, 0), and G2-M (n=15, 1, 0) durations of the daughter cells were quantified (n values corresponded to NCS 100 ng/mL, 200 ng/mL, 300 ng/mL). Control represents cells without NCS treatment. Error bars represent standard deviations.

E-F. Same as in A-B, but with U2OS cells.

G-H. Same as in C-D, but with U2OS. (G) For cells damaged in G1, the subsequent S (n=31, 36, 32) and G2-M (n=26, 25, 17) durations were quantified. (H) For cells damaged in G2-M, the G1 (n=51, 28, 8), S (n=38, 25, 6), and G2-M (n=32, 11, 5) durations of the daughter cells were quantified (n values corresponded to NCS 100 ng/mL, 200 ng/mL, 300 ng/mL).

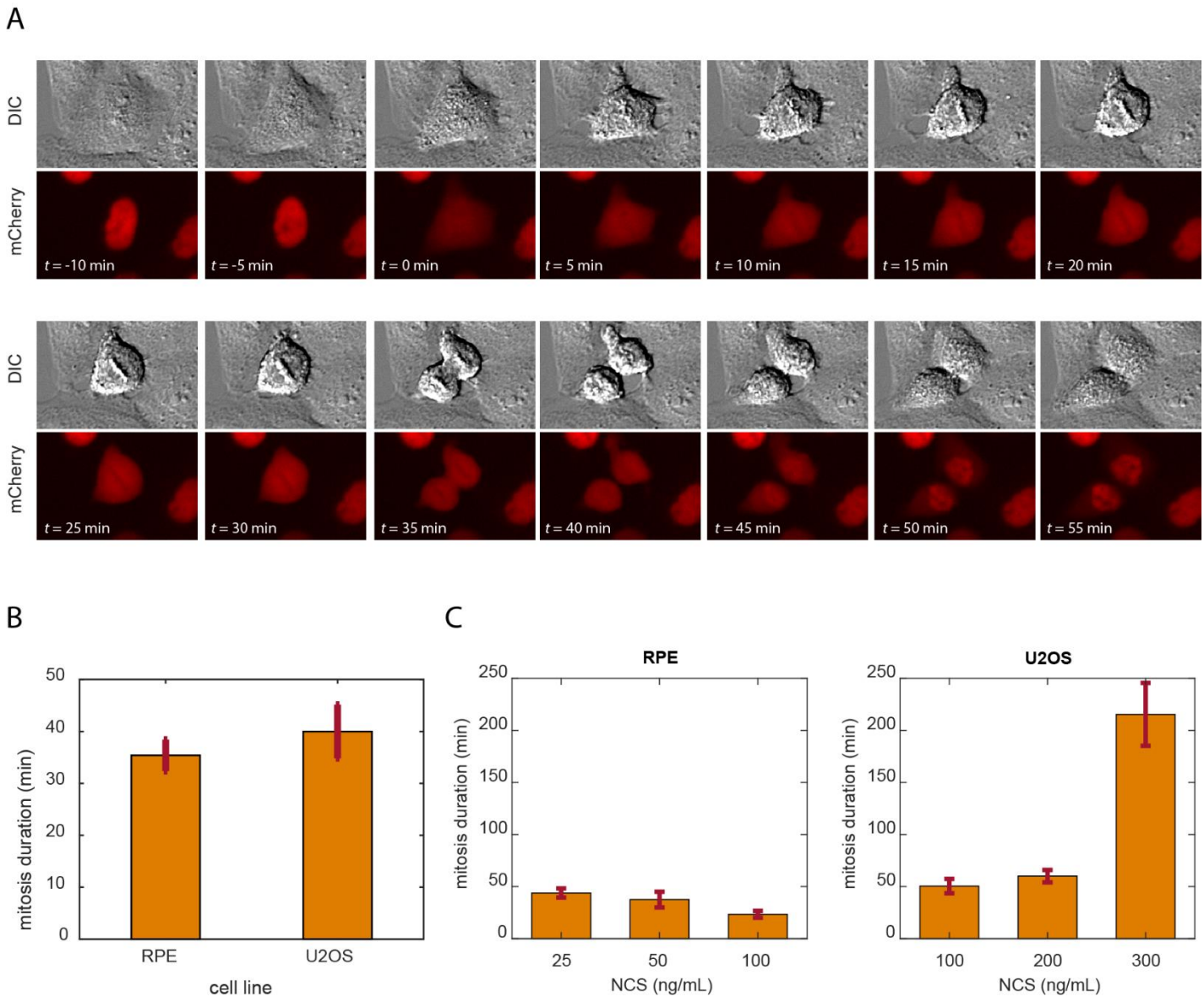

Figure S14. Mitosis durations of RPE and U2OS cells.

A. Live-cell images of a single U2OS cell undergoing mitosis. Upper row: differential interference contrast (DIC). Lower row: mCherry channel. t represents the time since the onset of mitosis, identified by cell rounding and nuclear envelop breakdown.

B. Mitosis durations based on nuclear envelope breakdown revealed by both DIC and mCherry channels under basal conditions. The error bars represent standard error of mean (n=10).

C. Mitosis durations based on nuclear envelope breakdown revealed by both the DIC and mCherry channels under basal conditions. The error bars represent standard error of mean (RPE: n=31 (25 ng/mL), 4 (50 ng/mL), 3 (100 ng/mL). U2OS: n>32 in all conditions).

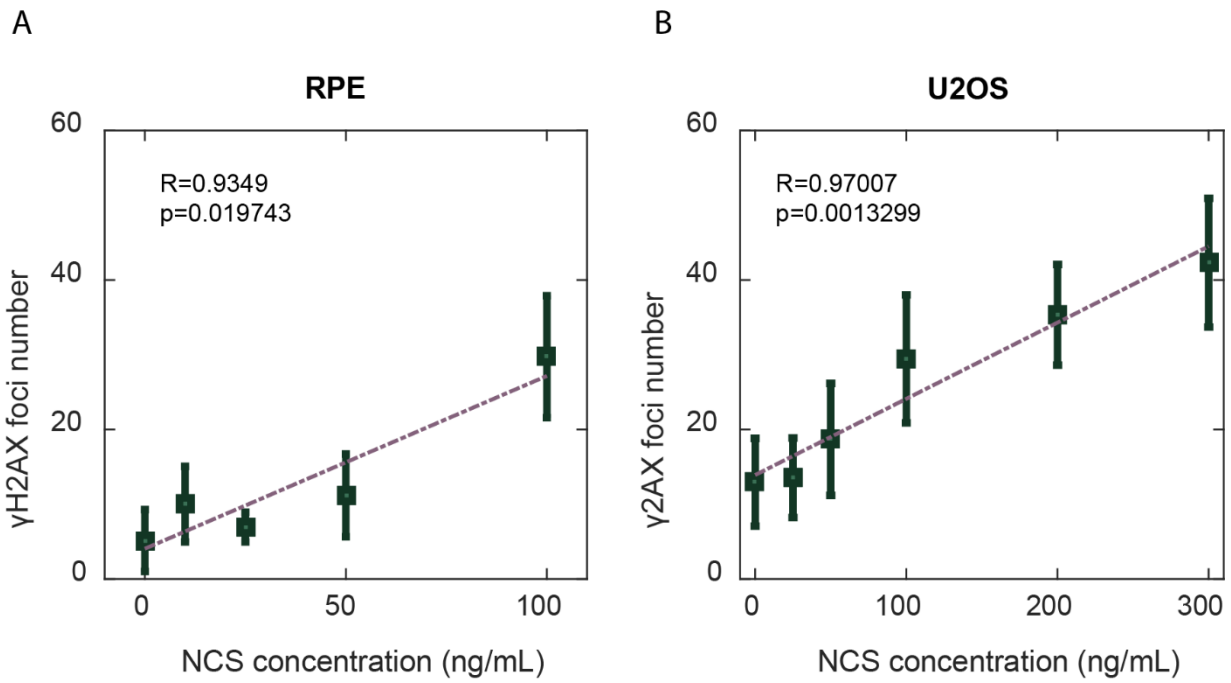

Figure S15. Linear relationship between NCS concentrations and γH2AX foci number in (A) RPE and (B) U2OS cells. Asynchronous cells were treated with the indicated concentrations of NCS. After 60 minutes, cells were fixed, stained, and quantified for γH2AX foci. The data were fitted with a linear regression. The error bars represent standard error of the mean.

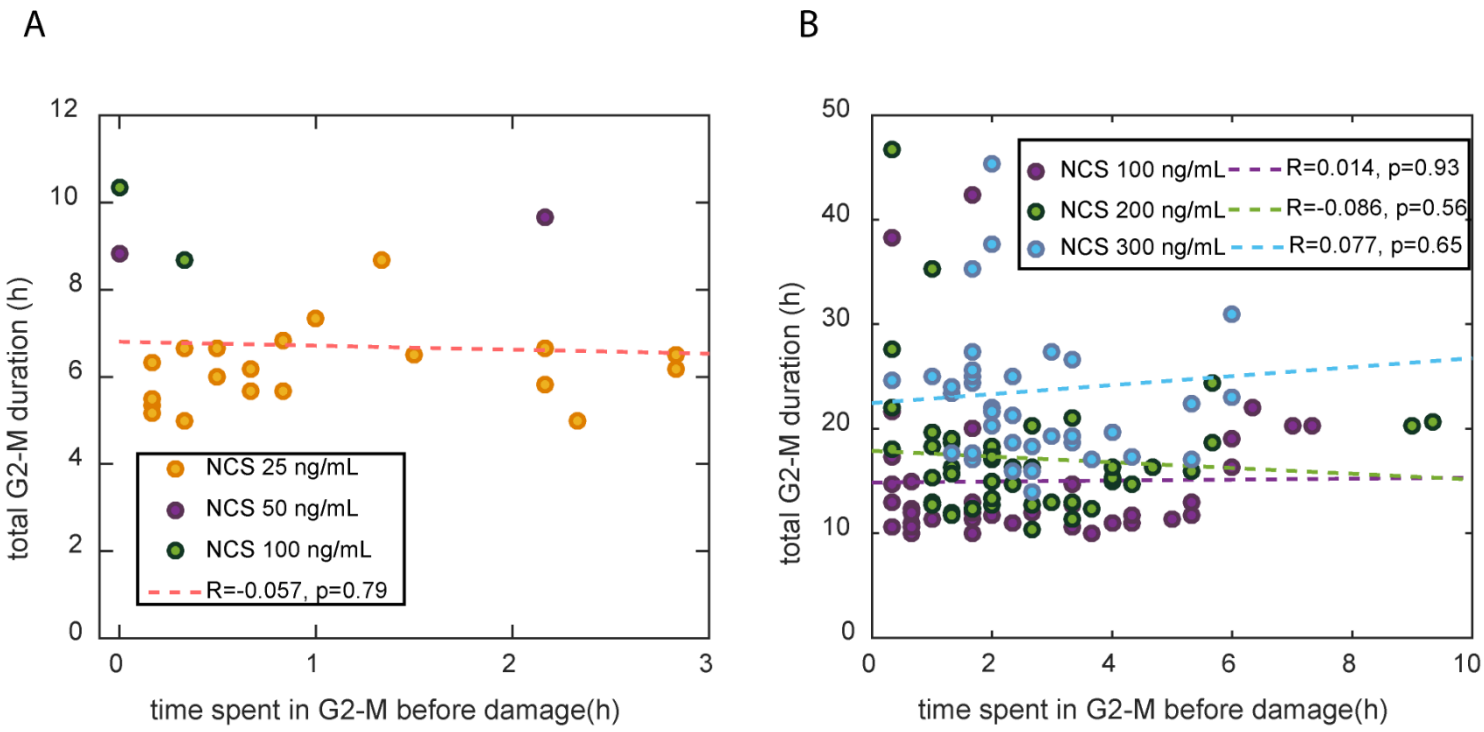

Figure S16. The halt durations imposed in G2-M were independent of the timing of DNA damage throughout the cell cycle phase. (A) RPE and (B) U2OS cells were treated with the indicated NCS concentrations and followed for phase transitions. The total G2-M durations were plotted against the time spent in G2-M before damage. The data were fitted with a linear regression. The data for RPE under 50 ng/mL and 100 ng/mL were not fitted with linear regression separately, due to the small sample size.

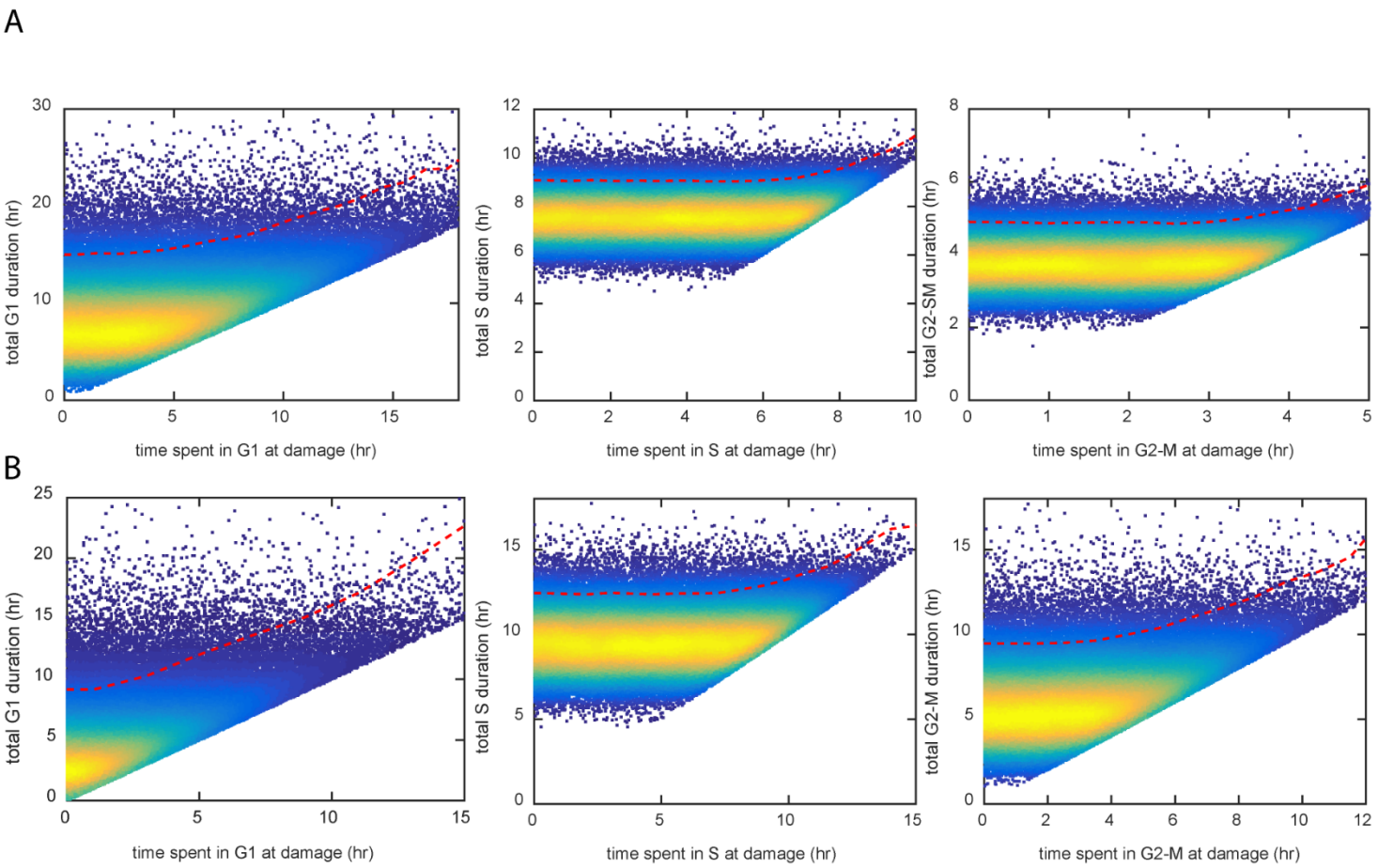

Figure S17. Simulation of cell cycle phase duration produced the 95 percentile cell cycle. Simulation parameters were obtained from the untreated controls' cell cycle phase durations of (A) RPE and (B) U2OS, fitted with the Erlang distribution. Each point represents a single simulated cell, and the colors represent the density of data points. The red dashed lines represent the top 95 percentile of the total S phase duration for a given time spent in that phase at damage.

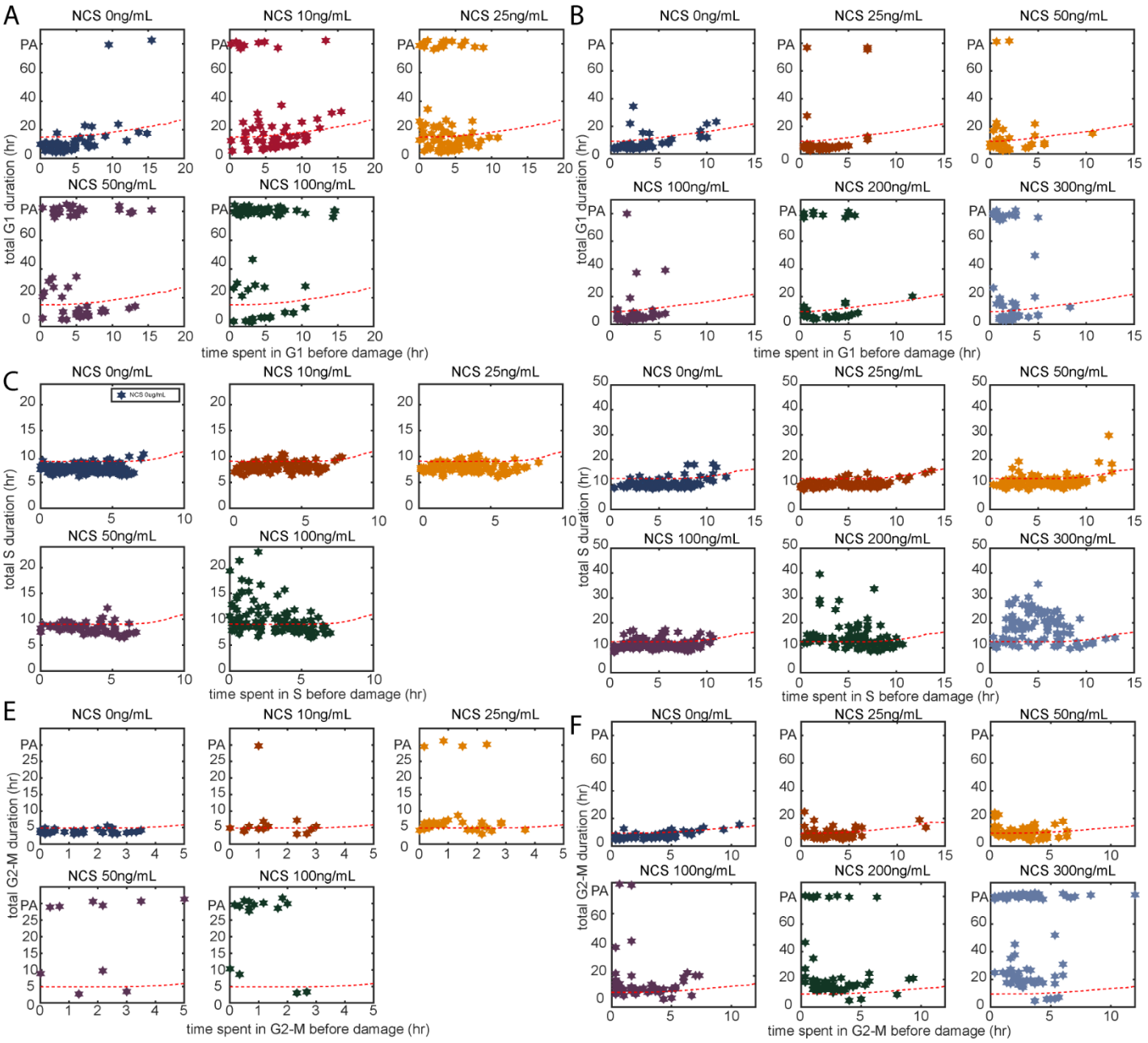

Figure S18. Cell cycle response as a function of cell cycle progress into the phase of damage in (A, C, E) RPE and (B, D, F) U2OS. The total cell cycle phase durations were plotted against the time spent in that phase at the time of damage. The 95 percentile lines (red dashed lines) obtained from **Figure S17** were superimposed onto these plots. This analysis allows for the designation each cell into the three outcome categories (unaffected, temporary arrest, and permanent arrest), as in **Figure 5B**. PA indicates permanent arrest.

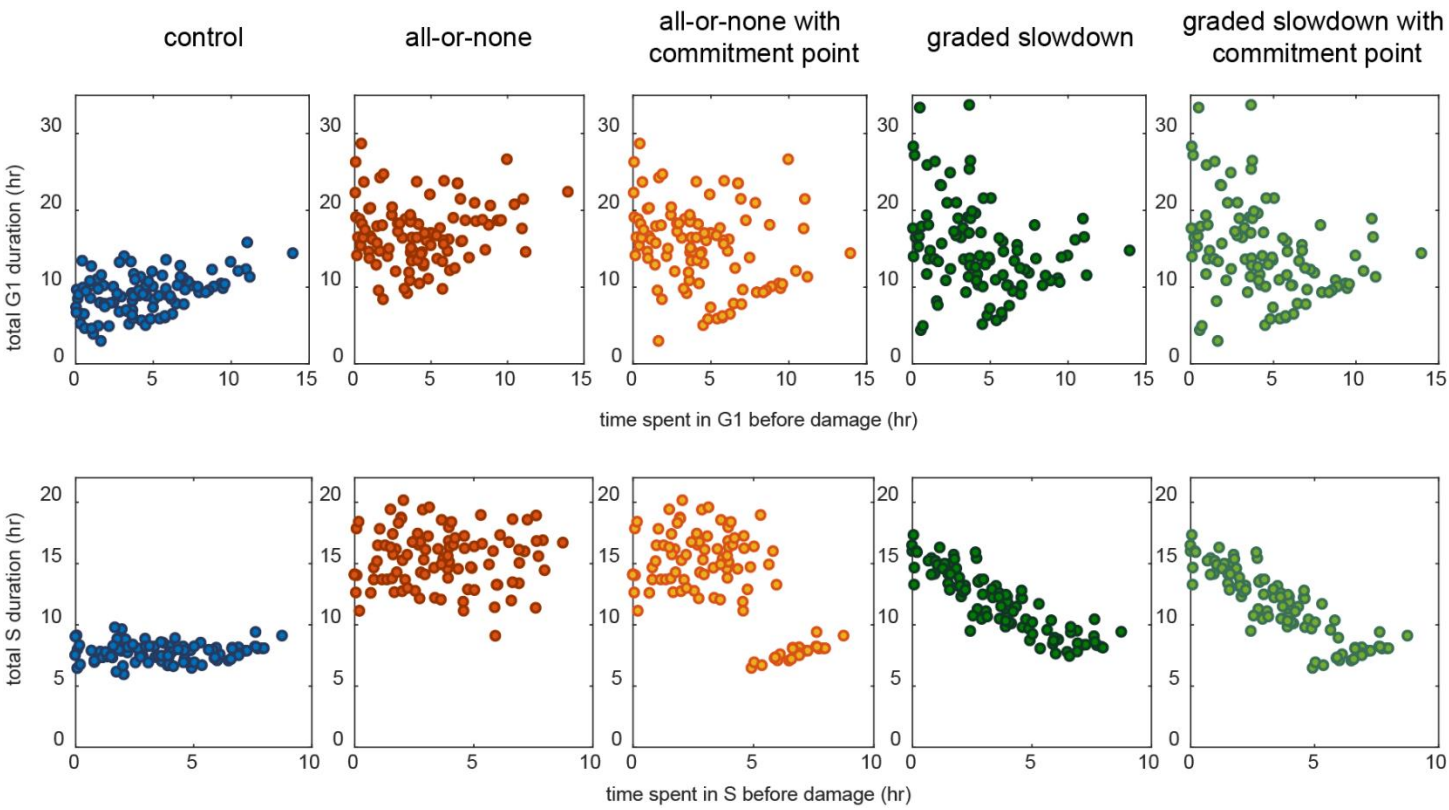

Figure S19. Model simulation demonstrating the timing of DNA damage within cell cycle phase stage affects the total phase duration.

Simulations of cell cycle phase durations as a function of time spent in that phase before damage. Simulations were performed using the fitted parameters (the shape, *k*, and scale, 1/λ) from RPE's G1 and S phase distributions to represent a phase duration with large variance and small variance, respectively. In the cases with all-or-none checkpoint kinetics, the delay duration was 8 hours. In the cases of graded slowdown checkpoint kinetics, the slowdown factor was 0.5. In the cases of an internal commitment point, the location was 75% of the entire phase from the onset of the phase.

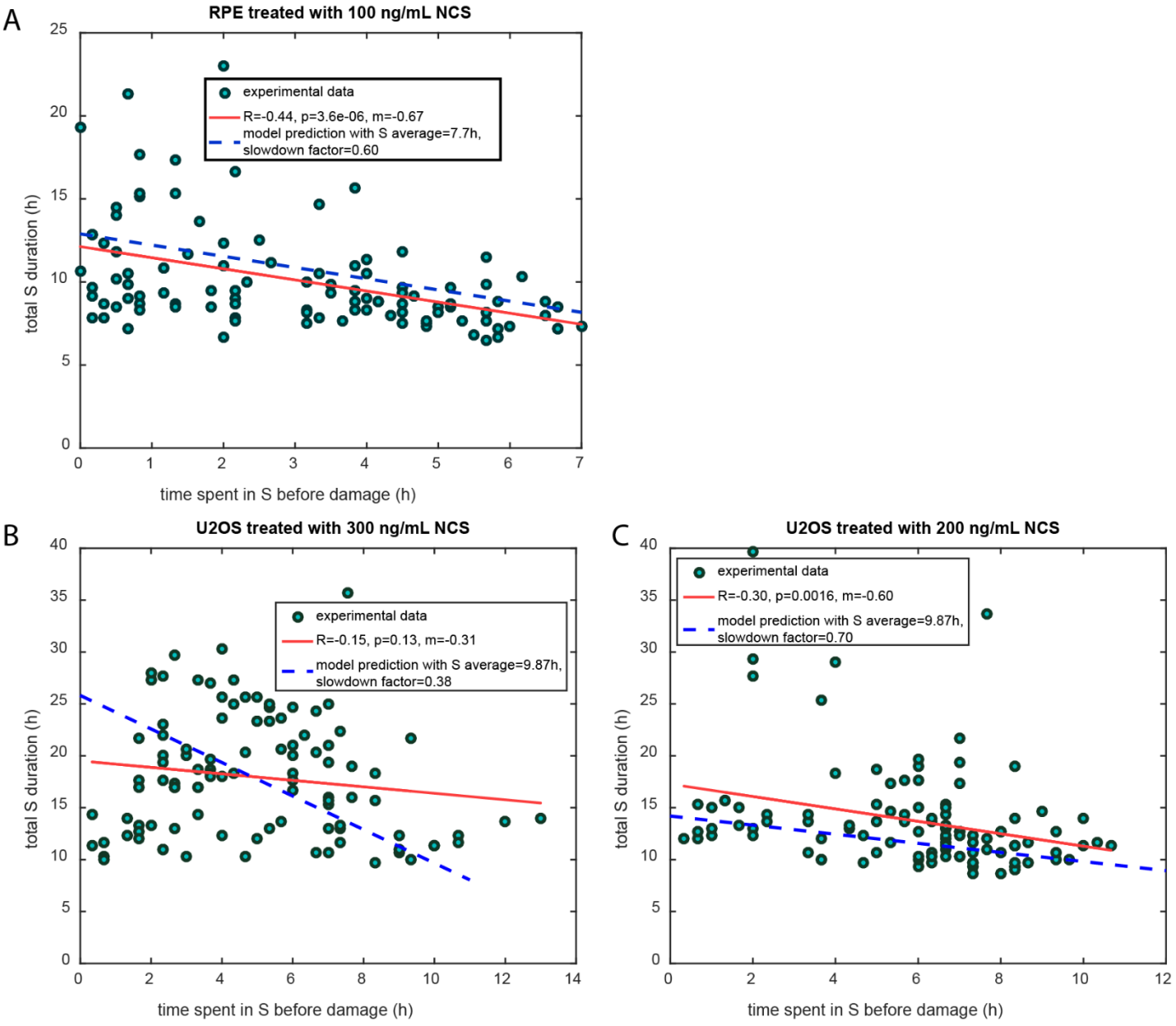

Figure S20. The delay in S phase completion linearly depends on the timing of DNA damage within S phase.

Experimental data of the total S phase durations as a function of time spent in S phase before damage. Red lines represent linear regression of the experimental data. Blue dash lines represent the model predictions of the mean S phase durations based on the graded slowdown checkpoint kinetics.

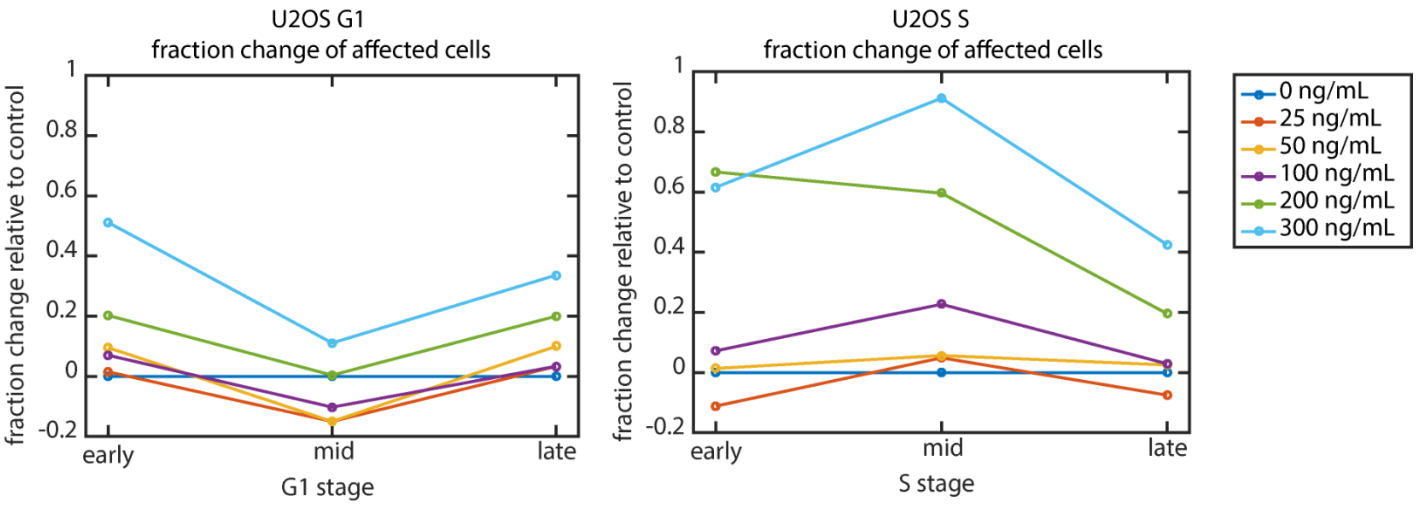

Figure S21. Cell cycle outcomes in response to DSBs depend on cell cycle phases and stages within each phase.

Cell cycle outcome's dependency on the stage of cell cycle phase progression, as in **Figure 6C**. Cell cycle outcomes are plotted as a function of cell cycle phase stage—early, mid, and late stages. Early, mid, and late stages were categorized based on thresholds defined by the 33 and 67 percentiles of time spent in a phase at the time of damage. Fraction change relative to control was obtained by calculating the difference between the fraction of cells being affected (either temporary or permanent arrest) under NCS treatment and that without NCS treatment. The construction of such cell cycle phase stage plot in RPE's G2-M could not be performed due to the short length of G2-M duration and sparsity of cells (see **Figure S18E**). The increased affected fraction in late G1 stage can be explained by sampling bias, such that cells categorized as late stage were possibly already activating arrest response before NCS treatment. Therefore, there is a strong dependency of total duration on the stage during which the cell is sampled, as seen in **Figure S17B** left panel.

Table 1. Fitting parameters for the "arrest-and-restart" checkpoint model.

G1			
	NCS (ng/mL)	**time delay (h)**	**permanent arrest probability**
	0	0.4932	0.0252
	10	1.8399	0.2147
	25	1.7891	0.2333
	50	0.0864	0.4596
RPE	100	0.1242	0.6717
	0	0.7872	0.0221
	25	0.075	0.0738
	50	1.3993	0.0611
	100	0.4638	0.0553
	200	9.31E-01	0.2281
U2OS	300	0.9816	0.311
S			
	NCS (ng/mL)	**time delay (h)**	**permanent arrest probability**
	0	0.4093	0.0028
	10	0.5294	0.0042
	25	0.2848	2.96E-04
	50	0.7645	9.34E-04
RPE	100	2.3355	0.0213
	0	3.06E-04	1.79E-04
	25	4.89E-01	5.47E-05
	50	0.5125	1.87E-04
	100	1.8002	2.49E-04
	200	2.2	0.0099
U2OS	300	6.75	0.0093
G2-M			
	NCS (ng/mL)	**time delay (h)**	**permanent arrest probability**
	0	0.3022	3.59E-04
	10	1.0622	0.0456
	25	2.1987	0.1081
	50	5.0812	0.5414
RPE	100	4.9552	0.7361
	0	4.98E-01	0.0104
	25	1.6519	0.0105
	50	3.4003	0.0112
	100	6.5444	0.0726
	200	9.3505	0.1656
U2OS	300	0.9816	0.311

Table S2. Fitting parameters for the refined checkpoint model with all-or-none kinetics.

G1					
	NCS (ng/mL)	**time delay (h)**	**permanent arrest probability**	**commitment point (fraction from phase onset)**	**difference between data and model**
RPE	**0**	0.5059	0.0592	0.6047	0.074
	10	8.7336	0.2941	0.5104	0.2291
	25	8.8012	0.3824	0.5084	0.3027
	50	16.5	0.72	0.52	0.0547
	100	22.0196	0.818	0.7484	0.0351
U2OS	**0**	5.29E-01	2.13E-05	0.9496	0.1222
	25	9.04E-05	0.0993	0.6333	0.0542
	50	2.2204	0.0922	0.6758	0.1748
	100	0.9751	0.1489	0.3506	0.0933
	200	4.00E+00	0.4	0.5139	0.0879
	300	7.8327	0.5694	0.5036	0.249
S					
	NCS (ng/mL)	**time delay (h)**	**permanent arrest probability**	**commitment point (fraction from phase onset)**	**difference between data and model**
RPE	**0**	0.5988	0.0026	0.9648	0.0195
	10	0.7661	1.20E-03	0.9976	0.1123
	25	0.3742	1.40E-03	9.99E-01	3.82E-02
	50	0.6504	1.40E-03	9.98E-01	2.82E-02
	100	2.3799	9.54E-04	0.9974	0.52
U2OS	**0**	2.23E-05	1.89E-05	0.7009	0.0823
	25	1.05E+00	8.77E-20	1.00E+00	3.98E-02
	50	8.42E-08	1.01E-02	0.0967	0.016
	100	1.9833	1.53E-04	0.8988	0.0371
	200	4.0074	0.04	0.4002	0.1035
	300	8.5809	0.031	0.897	0.1367
G2-M					
	NCS (ng/mL)	**time delay (h)**	**permanent arrest probability**	**commitment point (fraction from phase onset)**	**difference between data and model**
RPE	**0**	0.2606	1.40E-03	0.7178	0.0258
	10	1.45	0.0543	0.7621	0.0723
	25	2.294	0.121	0.9057	0.0667
	50	6.0419	0.651	0.8184	0.0642
	100	6	0.81	0.88	0.0551
U2OS	**0**	1.05E+00	2.50E-04	0.9995	0.0932
	25	1.9333	9.70E-03	8.53E-01	0.0547
	50	3.2045	1.00E-02	0.8774	0.0575
	100	6.58	0.0731	0.9554	0.0706
	200	9.3695	0.178	0.9573	0.0554
	300	15.1824	0.5423	0.9587	0.0308

Table S3. Fitting parameters for the refined checkpoint model with graded slowdown kinetics.

G1					
	NCS (ng/mL)	**slowdown factor**	**permanent arrest probability**	**commitment point (fraction from phase onset)**	**difference between data and model**
	0	0.952	0.0191	0.9999	0.0487
	10	0.5832	0.157	0.9581	0.2804
	25	0.5795	0.2008	0.9998	0.1297
	50	0.2573	0.6969	0.594	0.0868
RPE	**100**	0.3313	0.7971	0.7878	0.076
	0	0.71	1.25E-04	0.9999	0.1167
	25	0.1112	0.194	0.0989	0.0425
	50	0.5121	0.047	0.8961	0.0487
	100	0.2093	2.95E-01	0.0978	0.039
	200	6.80E-01	0.2175	0.9999	0.0479
U2OS	**300**	0.51	0.288	0.9998	0.1006
S					
	NCS (ng/mL)	**slowdown factor**	**permanent arrest probability**	**commitment point (fraction from phase onset)**	**difference between data and model**
	0	0.95	2.30E-04	0.9699	0.0362
	10	0.9077	9.21E-05	0.9705	0.2602
	25	0.9061	2.50E-04	9.70E-01	6.66E-02
	50	0.9059	2.70E-04	9.70E-01	2.51E-02
RPE	**100**	0.5971	3.76E-04	0.9614	0.119
	0	0.9022	2.50E-04	0.1015	0.1106
	25	0.9	5.72E-08	1.00E+00	5.48E-02
	50	0.9015	5.84E-05	0.8971	0.0202
	100	0.8076	4.48E-07	0.9	0.0695
	200	0.6952	1.49E-05	0.9998	0.0826
U2OS	**300**	0.3823	3.34E-04	0.9997	0.1123
G2-M					
	NCS (ng/mL)	**slowdown factor**	**permanent arrest probability**	**commitment point (fraction from phase onset)**	**difference between data and model**
	0	0.9042	1.25E-05	0.99	0.0284
	10	0.6929	0.0599	0.9488	0.1943
	25	0.5034	0.104	0.9999	0.1751
	50	0.2945	0.6061	0.8974	0.1301
RPE	**100**	0.2855	0.8166	0.8792	0.0631
	0	0.7979	2.59E-04	0.9999	0.2536
	25	0.604	2.08E-04	0.9023	0.043
	50	0.4904	1.44E-04	1.00E+00	0.1152
	100	0.3144	0.0292	0.8998	0.5278
	200	0.3103	0.1499	1	0.9916
U2OS	**300**	0.0994	0.25	1	0.3046